Taylor & Francis
Taylor & Francis Group

ORIGINAL ARTICLE

OPEN ACCESS

Escherichia coli γ-carbonic anhydrase: characterisation and effects of simple aromatic/heterocyclic sulphonamide inhibitors

Sonia Del Prete[a] (iD), Silvia Bua[b], Claudiu T. Supuran[b] (iD) and Clemente Capasso[a] (iD)

[a]Department of Biology, Agriculture and Food Sciences, CNR, Institute of Biosciences and Bioresources, Napoli, Italy; [b]Section of Pharmaceutical and Nutraceutical Sciences, Department of NEUROFARBA, University of Florence, Firenze, Italy

ABSTRACT

Carbonic anhydrases (CAs, EC 4.2.1.1) are ubiquitous metalloenzymes involved in biosynthetic processes, transport, supply, and balance of CO_2/HCO_3^- into the cell. In Bacteria, CAs avoid the depletion of the dissolved CO_2/HCO_3^- from the cell, providing them to the central metabolism that is compromised without the CA activity. The involvement of CAs in the survival, pathogenicity, and virulence of several bacterial pathogenic species is recent. Here, we report the kinetic properties of the recombinant γ-CA (EcoCAγ) encoded in the genome of *Escherichia coli*. EcoCAγ is an excellent catalyst for the physiological CO_2 hydration reaction to bicarbonate and protons, with a k_{cat} of $5.7 \times 10^5 \, s^{-1}$ and k_{cat}/K_M of $6.9 \times 10^6 \, M^{-1} \, s^{-1}$. The EcoCAγ inhibition profile with a broad series of known CA inhibitors, the substituted benzene-sulphonamides, and clinically licenced drugs was explored. Benzolamide showed a K_I lower than 100 nM. Our study reinforces the hypothesis that the synthesis of new drugs capable of interfering selectively with the bacterial CA activity, avoiding the inhibition of the human α-CAs, is achievable and may lead to novel antibacterials.

1. Introduction

Nature developed a fascinating system for recycling CO_2[1,2]. Plant, algae, and photosynthetic prokaryotes through the photosynthetic process can convert light energy into chemical energy[1]. The last is stored in the carbohydrates, and the carbon dioxide (CO_2) is fixed into biomass. In the aerobic environment, carbon from the biomass returns to the atmosphere by the action of O_2-requiring decomposers, such as bacteria and fungi[3], while, in an environment characterised by the absence of oxygen, the anaerobic microbes decompose the biomass releasing methane and CO_2[4]. The carbon cycle is essential for the life on the Earth since carbon is a critical component in controlling the planet temperature, a crucial food ingredient for sustaining the entire living organisms, and, finally, an energy source for driving the global economy[5]. A necessary enzyme involved in the carbon cycle, which has the function to enhance the photosynthesis via a mechanism that concentrates and supplies CO_2 up to 1000-fold close to the ribulose-1,5-bisphosphate carboxylase (RuBisCO), is the carbonic anhydrase (CA, EC 4.2.1.1) [6]. Several CA-classes have been identified, such as α, β, γ, δ, ζ, η, θ, and ι[7–9]. The eight CA-classes, showing a low sequence similarity, different folds and structures, are considered phylogenetically distinct. This exceptional sequence and structural divergence evolved, reflecting a convergent evolution of the CA-classes since they target a common substrate, the CO_2, and catalyse the same reaction, the simple but physiologically crucial reaction of carbon dioxide hydration/dehydration to bicarbonate and protons ($CO_2 + H_2O \rightleftarrows HCO_3^- + H^+$)[10–17]. The CO_2 hydratase reaction is catalysed at very high rates, with a pseudo-first-order kinetic constant (k_{cat}) ranging from 10^4 to $10^6 \, s^{-1}$ (18, 19), which is about 67,000–7,000,000 times higher than the uncatalyzed reaction with a $k_{cat} = 0.15 \, s^{-1}$[18,19]. In addition to the involvement in photosynthetic processes, CAs accomplish the transport, supply, and balance of CO_2 and bicarbonate into the cell, but also pH homeostasis, secretion of electrolytes, and participate in several biosynthetic processes[20,21]. The homeostasis of H^+ and CO_2/HCO_3^- is involved in many physiological and pathological conditions[18,19,22–26]. In Bacteria, for example, the primary CA function is to avoid the depletion of the dissolved inorganic carbon (CO_2/HCO_3^-) from the cell, providing them quickly to the central metabolism, which might be compromised without the CA activity[7,8,16,27–29]. A charming example is represented by the β-CA (CynT) encoded by the genome of the bacterium *Escherichia coli*, a Gram-negative bacterium typically colonising the lower intestine of warm-blooded organisms[30–32]. The *E. coli* cyn operon contains three genes, CynT, CynS, and CynX encoding for a β-CA, a cyanase, and an unknown protein, respectively[33]. CynT catalysing the CO_2 hydration produces HCO_3^-, whose depletion from the bacterial cells is avoided since the cyanase uses it as a substrate to produce ammonia and CO_2[33–35].

Numerous examples support the importance of CA activity in the growth of bacteria. For example, the deletion of a gene encoding for the β-CA from *Ralstonia eutropha* allowed the heterotrophic growth of the mutant only at an elevated concentration of CO_2 compared to wild-type[36]. In *E. coli*, a second β-CA, CynT2, is essential for the growth of the microorganism at atmospheric pCO_2[37,38]. The lost of CA genes in some Proteobacteria,

such as those belonging to the genera Buchnera and Rickettsia, determined their adaptation only in high-CO$_2$ niches[39]. More interesting, are the discovery of the involvement of CAs in the survival, pathogenicity, and virulence of several species of human pathogens, such as *Helicobacter pylori*[40–42], *Vibrio cholerae*[43], *Brucella suis*[44–47], *Salmonella enterica*[48], and *Pseudomonas aeruginosa*[49] among others.

In this context, we focalised our interest in the inhibition profile of the CAs encoded by the genome of *E. coli*, a bacteria generally coexisting in a mutually beneficial state with the host[50]. In some cases, it may become a severe pathogen[51–53] or can cause diseases if the host defences are weakened[54]. The *E. coli* genome encodes for β-CAs (Cyn T and CynT2), γ- and ι-CAs. Here, we cloned, overexpressed, and purified the γ-CA (EcoCAγ) enzyme. The recombinant EcoCAγ was subjected to the investigation of its kinetic properties since only the three-dimensional structure was determined in 2012[55]. Besides, we explored the EcoCAγ inhibition profile with a broad series of substituted benzene-sulphonamides and clinically licenced drugs, which generally inhibit the CAs in the nanomolar range[56–58]. The EcoCAγ inhibition profile was compared with those obtained for the two human isoforms (hCA I and hCA II) with the prospect of gaining new scientific knowledge in the design of potentially new inhibitors capable of blocking efficiently and selectively the CA activity encoded by the pathogenic microbes.

2. Materials and methods

2.1. Chemicals and instruments

All the chemicals used in this study were of reagent grade and purchased from Sigma. The Affinity column (His-Trap FF) and the AKTA-Prime purification system were bought from GE Healthcare. The SX20 Stopped-Flow and SDS–PAGE and Western-Blot apparatus were obtained by AppliedPhotophysics and BioRAD, respectively.

2.2. Cloning, expression and purification of the recombinant E.coli γ-CA

The synthetic *E. coli* gene encoding for the EcoCAγ (Accession number: WP_009008373.1) was synthesised by the Invitrogen GeneArt (ThermoFisher Scientific), a company specialised in gene synthesis, and cloned into the expression vector pET100D-Topo/γ-CA. Briefly, the gene was designed to produce the recombinant EcoCAγ as fusion proteins with a tag containing nucleotides encoding for six histidines (His-Tag) at the amino terminus of neosynthetized recombinant protein. Competent *E. coli* BL21 (DE3) codon plus cells (Agilent) were transformed as described by Del Prete et al. [59]. Isopropyl β-D-1-thiogalactopyranoside (IPTG) at the concentration of 1 mM was added to the cellular culture to overexpress the recombinant EcoCAγ. After growth, the cells were harvested and disrupted by sonication. Cellular extract was purified using a nickel affinity column (His-Trap FF), which allows the interaction between the matrix functionalised with Ni^{2+} ions and the His-Tag at the N-terminus of the protein. The HisTrap column (1 ml) was equilibrated with 20 ml equilibration buffer (50 mM Tris, 20 mM imidazole and 150 mM sodium chloride, pH 7.5) at 1 ml/min. The supernatant from the cellular lysate was loaded onto the column at 1 ml/min, and eluted from the column by fluxing imidazole (300 mM) at a flow of 0.5 ml/min in a buffer composed of 50 mM Tris and 300 mM sodium chloride, pH 7.5. The recovered

EcoCAγ was 90% pure. The protein quantification was carried out by Bradford method (BioRAD) [60].

2.3. Enzyme activity for monitoring the EcoCAγ purification

The CA activity assay was performed as described by Capasso et al. [61]. Briefly, the assay was based on the monitoring of pH variation due to the catalysed conversion of CO$_2$ to bicarbonate. Bromothymol blue was used as the indicator of pH variation. The assay was performed at 0 °C and a CO$_2$-satured solution was used as substrate. The enzyme activity was calculated by measuring the time required for Bromothymol blue to change from blue to yellow. This time is inversely related to the quantity of enzyme present in the sample and allows the calculation of the Wilbur-Anderson units as described previously[61].

2.4. Sds-PAGE, protonography and Western-Blot

A 12% Sodium Dodecyl Sulfate-polyacrylamide gel electrophoresis (SDS-PAGE) prepared as described by Laemmli[62] was used, loading on the gel the recovered EcoCAγ from the affinity column. The gel was stained with Coomassie Brilliant Blue-R. To perform the protonography, wells of 12% SDS-PAGE gel were loaded with samples mixed with loading buffer not containing 2-mercaptoethanol and not subjected to boiling, in order to avoid protein denaturation. The gel was run at 150 V until the dye front ran off the gel. Following the electrophoresis, the 12% SDS-PAGE gel was subject to protonography to detect the yellows bands due to the hydratase activity on the gel as described previously[63–66]. In addition, EcoCAγ was transferred to a PVDF (polyvinylidene fluoride) membrane with transfer buffer (25 mM Tris, 192 mM glycine, 20% methanol) using Trans-Plot SD Cell (Bio-Rad, Hercules, CA, USA). His-Tag Western blot was carried out using the Pierce Fast Western Blot Kit (Thermo Scientific, Waltham, MA, USA). Blotted membrane was placed in the wash blot solution Fast Western 1 Wash Buffer to remove transfer buffer. Primary Antibody Working Dilution was added to the blot and incubated for 30 min at room temperature (RT) with shaking. Invitrogen anti-His antibody (1:10000) was used. Afterwards, the blot was removed from the primary antibody solution and incubated for 10 min with the FastWestern Optimised HRP ReagentWorking Dilution. Subsequently, the membrane was washed two times in about 20 ml of FastWestern 1Wash Buffer. Finally, the membrane was incubated with the detection reagent working solution and incubated for 1 min, at room temperature, and then developed with X-ray film.

2.5. Kinetic parameters and inhibition constants

The CO$_2$ hydration activity performed by the EcoCAγ was monitored using an Applied Photophysics stopped-flow instrument[67]. Phenol red (at a concentration of 0.2 mM) was used as indicator, working at the absorbance maximum of 557 nm, with 20 mM TRIS (pH 8.3) as buffer, and 20 mM NaClO$_4$ (for maintaining constant the ionic strength), following the initial rates of the CA-catalysed CO$_2$ hydration reaction for a period of 10–100 s. To determine the kinetic parameters by Lineweaver-Burk plots and the inhibition constants, a concentration of CO$_2$ between 1.7 to 17 mM was used. At least six measurements of the original 5–10% reaction were used to assess the initial velocity for each inhibitor. The uncatalyzed rates were identically determined and detracted from the total observed rates. Stock inhibitor solutions (10–100 mM)

```
1    ATG AAG TGT TTC ACG TTG TCG TCT CAA CGG AGG CGC ATT ATA GGG ATC CCA ATT TTT TGC    60 (nucleotide number)
1    M   K   C   F   T   L   S   S   Q   R   R   R   I   I   G   I   P   I   F   C     20 (amino acid number)
     TAC TTC ACA AAG TGC AAC AGC AGA GTT GCC TCC GCG TAA TAT CCC TAG GGT TAA AAA ACG

61   ACA AGT ACT TTT TTG ATC TTT TTT TCT GTT TGT TGT TTT TTC ACC CTT TTT GCT GCA TTC   120
21   T   S   T   F   L   I   F   F   S   V   C   C   F   F   T   L   F   A   A   F     40
     TGT TCA TGA AAA AAC TAG AAA AAA AGA CAA ACA ACA AAA AAG TGG GAA AAA CGA CGT AAG

121  GCA CAC AAA ACG GTG CTT TTT TGC ATA CTA AAA GAC TTG CAC AAG GCC AAT AAT GCC CCC   180
41   A   H   K   T   V   L   F   C   I   L   K   D   L   H   K   A   N   N   A   P     60
     CGT GTG TTT TGC CAC GAA AAA ACG TAT GAT TTT CTG AAC GTG TTC CGG TTA TTA CGG GGG

181  AAA GTC ATT AGT AAA TCA TTT ATT GCT GAG GTA AGT ATG TCT GAT GTT TTA CGC CCA TAC   240
61   K   V   I   S   K   S   F   I   A   E   V   S   M   S   D   V   L   R   P   Y     80
     TTT CAG TAA TCA TTT AGT AAA TAA CGA CTC CAT TCA TAC AGA CTA CAA AAT GCG GGT ATG

241  CGC GAT CTT TTT CCA CAA ATC GGT CAG CGC GTA ATG ATC GAC GAT AGC AGT GTC GTG ATT   300
81   R   D   L   F   P   Q   I   G   Q   R   V   M   I   D   D   S   S   V   V   I    100
     GCG CTA GAA AAA GGT GTT TAG CCA GTC GCG CAT TAC TAG CTG CTA TCG TCA CAG CAC TAA

301  GGT GAC GTT CGT CTG GCT GAT GAT GTG GGG ATC TGG CCG CTC GTT GTG ATT CGT GGA GAT   360
101  G   D   V   R   L   A   D   D   V   G   I   W   P   L   V   V   I   R   G   D    120
     CCA CTG CAA GCA GAC CGA CTA CTA CAC CCC TAG ACC GGC GAG CAA CAC TAA GCA CCT CTA

361  GTA CAT TAT GTA CAG ATC GGA GCA CGC ACC AAT ATC CAG GAT GGC AGT ATG TTG CAT GTC   420
121  V   H   Y   V   Q   I   G   A   R   T   N   I   Q   D   G   S   M   L   H   V    140
     CAT GTA ATA CAT GTC TAG CCT CGT GCG TGG TTA TAG GTC CTA CCG TCA TAC AAC GTA CAG

421  ACT CAT AAA TCC TCG TAC AAC CCA GAT GGC AAC CCA TTA ACC ATT GGC GAA GAT GTC ACT   480
141  T   H   K   S   S   Y   N   P   D   G   N   P   L   T   I   G   E   D   V   T    160
     TGA GTA TTT AGG AGC ATG TTG GGT CTA CCG TTG GGT AAT TGG TAA CCG CTT CTA CAG TGA

481  GTT GGT CAC AAG GTG ATG CTC CAC GGC TGC ACC ATT GGC AAT CGA GTT TTG GTT GGG ATG   540
161  V   G   H   K   V   M   L   H   G   C   T   I   G   N   R   V   L   V   G   M    180
     CAA CCA GTG TTC CAC TAC GAG GTG CCG ACG TGG TAA CCG TTA GCT CAA AAC CAA CCC TAC

541  GGC TCA ATT TTA CTT GAT GGC GCA ATA GTA GAA GAT GAT GTG ATG ATT GGT GCG GGT AGT   600
181  G   S   I   L   L   D   G   A   I   V   E   D   D   V   M   I   G   A   G   S    200
     CCG AGT TAA AAT GAA CTA CCG CGT TAT CAT CTT CTA CTA CAC TAC TAA CCA CGC CCA TCA

601  CTG GTC CCA CAA AAT AAA CGG CTG GAG AGC GGA TAT CTG TAT CTC GGT AGC CCC GTC AAA   660
201  L   V   P   Q   N   K   R   L   E   S   G   Y   L   Y   L   G   S   P   V   K    220
     GAC CAG GGT GTT TTA TTT GCC GAC CTC TCG CCT ATA GAC ATA GAG CCA TCG GGG CAG TTT

661  CAG ATC CGC CCG TTA AGT GAT GAA GAG AAG GCT GGG TTA CGT TAT TCC GCG AAT AAT TAC   720
221  Q   I   R   P   L   S   D   E   E   K   A   G   L   R   Y   S   A   N   N   Y    240
     GTC TAG GCG GGC AAT TCA CTA CTT CTC TTC CGA CCC AAT GCA ATA AGG CGC TTA TTA ATG

721  GTG AAA TGG AAA GAC GAA TAC CTG GAT CAG GGT AAC CAG ACC CAA CCT TGA                771
241  V   K   W   K   D   E   Y   L   D   Q   G   N   Q   T   Q   P   *               256
     CAC TTT ACC TTT CTG CTT ATG GAC CTA GTC CCA TTG GTC TGG GTT GGA ACT
```

Figure 1. Nucleotide and translated amino acid sequences of the EcoCAγ. The amino acid residues and the open reading frame are indicated by capital letters, in bold and not in bold, respectively, *, indicate the stop codon.

were prepared in distilled-deionized water and dilutions up to 0.01 mM were done with the buffer test. Inhibitor and enzyme solutions were preincubated together for 15 min at room temperature prior to assay, in order to allow for the formation of the E-I complex or for the eventual active site mediated hydrolysis of the inhibitor. The inhibition constants were obtained by non-linear least-squares methods using PRISM 6 and the Cheng-Prusoff equation, as reported earlier[12,14,68], and represent the mean from at

least three different determinations. h CAI and hCA II were recombinant enzymes obtained in-house.

3. Results and discussion

3.1. Primary structure analysis

Because the genome of *Escherichia coli* was full sequenced, it was designed and polymerised the synthetic gene encoding for the EcoCAγ polypeptide chain. The sequence of the synthetic gene and its corresponding protein are shown in Figure 1. The EcoCAγ nucleotide sequence consists of an open reading frame of 771 nucleotides, encoding for a polypeptide chain of 256 amino acid residues (Figure 1). The EcoCAγ was aligned with the YrdA amino acid sequence, which corresponded to the γ-CA crystallised in 2012 (55). As shown in Figure 2, EcoCAγ has the same polypeptide chain of the YrdA protein, except for the presence of 72 additional amino acids at the N-terminus. In bacteria genes are often found in a cluster on the chromosome, which are under control of a single promoter[69]. This gene organisation is known as an operon. Thus, it is possible that the additional 72 residues belong to a different protein encoded by the *E. coli* operon, which includes the gene encoding for the E.coli γ-CA, too. As described in the literature, γ-CA is a homotrimer with three zinc-containing active sites located at the interfaces between two monomers[55]. Each monomer is structurally characterised by a tandemly-repeated hexapeptide, which mostly shows an aliphatic residue, usually Ile, Val, or Leu, at the first position, a well-conserved residue is glycine at position two, and a residue Ala, Ser, Cys, Val, Thr, or Asn at position five (Figure 2) [70]. This repeated hexapeptide is essential for the left-hand fold of the trimeric β-helix structures, which contradistinguish the canonical γ-CAs and putative acetyltransferases/acyltransferases[55]. YrdA was crystallised without the extra 72 residues at the N-terminus because the authors considered only the polypeptide chain with the conserved hexapeptide-repeat motifs (182 amino acid residues), which generally typify all the γ-CA sequences (Figure 2).

Next paragraphs report 1) the heterologous expression and purification of the EcoCAγ full amino acid sequence (containing the extra 72 residues at the N-terminus of the polypeptide chain); 2) the determination of the kinetic parameters of EcoCAγ using the stopped-flow technique; and 3) the inhibition profile of EcoCAγ with a broad range of small molecules, which generally inactivate this class of enzyme.

3.2. Heterologous expression and purification

IPTG ((Isopropyl β-D-1-thiogalactopyranoside) induction of *E. coli* BL21 (DE3) cells transformed with the expression plasmid
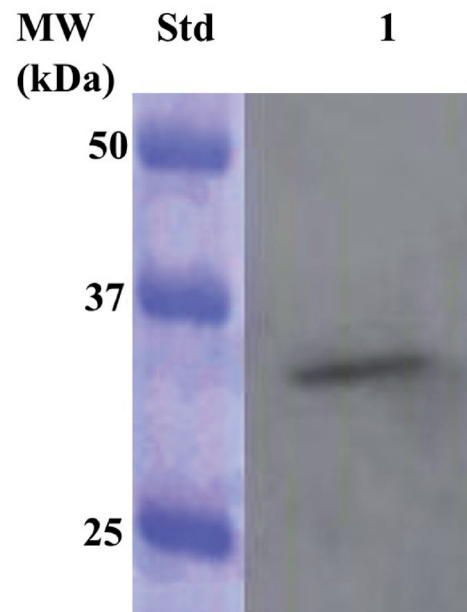

Figure 3. Western blot analysis performed on the supernatant coming from the *E. coli* cellular extract obtained after the sonication and centrifugation. Lane STD, molecular markers, M.W. starting from the top: 50 kDa, 37 kDa, and 25 kDa; lane 1, overexpressed chimeric EcoCAγ.

```
EcoCAγ      MKCFTLSSQRRRIIGIPIFCTSIFLIFFSVCCFFTLFAAIAHKTVLFCILKDLHKANNAP      60

YrdA        ------------------------------------------------------------

        61  KVISKSFIAEISMSDVLRPYRDLFPQIGQRVMIDDSSVVIGDVRLADDVGIWPLVVIRGD     120
                        MSDVLRPYRDLFPQIGQRVMIDDSSVVIGDVRLADDVGIWPLVVIRGD
         1  ------------MSDVLRPYRDLFPQIGQRVMIDDSSVVIGDVRLADDVGIWPLVVIRGD      48

       121  VHYVQIGARTNIQDGSMLHVTHKSSYNPDGNPLTIGEDVTVGHKVMLHGCTIGNRVLVGM     180
            VHYVQIGARTNIQDGSMLHVTHKSSYNPDGNPLTIGEDVTVGHKVMLHGCTIGNRVLVGM
        49  VHYVQIGARTNIQDGSMLHVTHKSSYNPDGNPLTIGEDVTVGHKVMLHGCTIGNRVLVGM     108

       181  GSILLDGAIVEDDVMIGAGSLVPQNKRLESGYLYLGSPVKQIRPLSDEEKAGLRYSANNY     240
            GSILLDGAIVEDDVMIGAGSLVPQNKRLESGYLYLGSPVKQIRPLSDEEKAGLRYSANNY
       109  GSILLDGAIVEDDVMIGAGSLVPQNKRLESGYLYLGSPVKQIRPLSDEEKAGLRYSANNY     168

       241  VKWKDEYLDQGNQTQP     256
            VKWKDEYLDQGNQTQP
       169  VKWKDEYLDQGNQTQP     184
```

Figure 2. Pairwise comparison of EcoCAγ amino acid sequence with the YrdA polypeptide chain. The pairwise alignment was performed with the programme Blast Global Align. The accession numbers of the aligned sequences are WP_009008373.1 (EcoCAγ) and P0A9W9 (YrdA). Legend: The extra 72 amino acid residues are in green bold; the identical amino acid residues are between the two aligned sequences; the amino acid residues of a typically repeated hexapeptide are reported in bold blue; the three histidines coordinating the metal ion are in red bold; the catalytically relevant residues, which participate in a network of hydrogen bonds with the catalytic water molecule, are represented in black bold; a hyphen shows gaps.
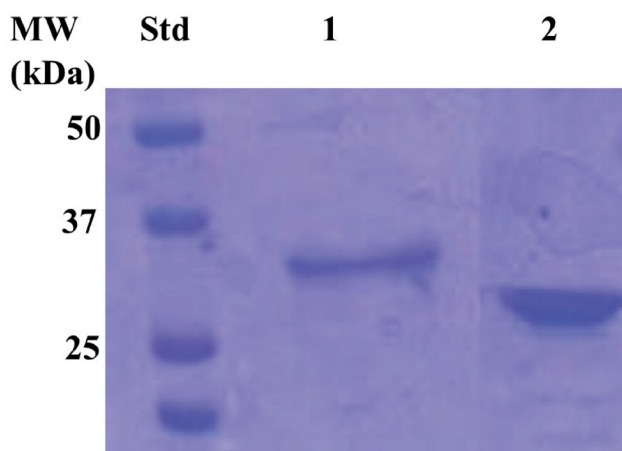
Figure 4. Electropherogram of the SDS-PSAGE carried out on the recombinant chimeric EcoCAγ. Legend: lane STD, molecular markers, M.W. starting from the top: 50 kDa, 37 kDa, and 25 kDa; lane 1, chimeric EcoCAγ; Lanes 2 commercial bovine CA (bCA) used as control. The band at a molecular weight of about 33.0 kDa represented the chimeric EcoCAγ purified by affinity chromatography.
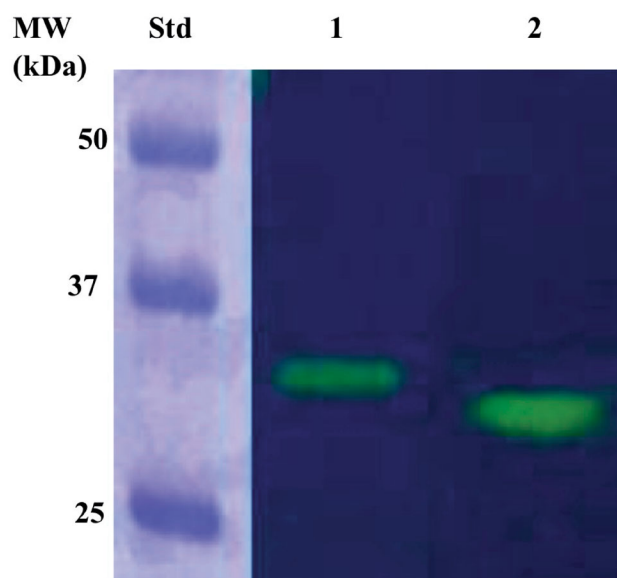

Figure 5. Protonogram of the EcoCAγ eluted from the affinity resin. The yellow band on the protonogram corresponds to the enzyme activity responsible for the drop of pH from 8.2 to the transition point of the dye in the control buffer (pH 6.8), due to the hydratase activity. Lane STD, molecular markers starting from the top: 50 kDa, 37 kDa, and 25 kDa; Lane 2, purified EcoCAγ; Lane 3, commercial bovine CA (bCA) used as a positive control.

containing the complete EcoCAγ gene resulted in the production of the recombinant γ-CA as a chimeric polypeptide chain obtained by the fusion of the N-terminus of the EcoCAγ protein to the C-terminus of a soluble peptide (about 4.0 kDa) containing six histidines (His-Tag). This strategy has been adopted to improve the solubility, purification, and detection of the recombinant EcoCAγ expressed in its complete form (plus the extra 72 residues at the N-terminus). After the sonication and centrifugation, most of the CA activity was recovered in the soluble fraction of the *E. coli* cell extract. The expression of the chimeric EcoCAγ was confirmed by Western Blot (WB) analysis using an anti-His-Tag antibody (Figure 3). As expected, analysing the *E. coli* cellular extract, the specific antibody for the His-Tag tail recognised the fusion protein as a band with a molecular weight of about 33.0 kDa. A subunit molecular mass of 32.4 kDa was calculated on the amino acid sequence translated from the chimeric gene encoding for the chimeric EcoCAγ.

The recombinant enzyme was purified to homogeneity using the affinity chromatography, as demonstrated by the SDS-Page analysis (Figure 4). As a result, the electropherogram profile of EcoCAγ showed a band at the same position identified in the western-blot analysis (33.0 kDa) under reducing conditions (Figure 4).

The full sequence of the recombinant EcoCAγ was also subjected to protonography, a powerful and elegant technique able to reveal, as a yellow band on the polyacrylamide gel, the production of ions (H^+) developed during the CO_2 hydration reaction[63,65]. The protonography analysis demonstrated that the complete EcoCAγ polypeptide chain was catalytically active. The protonogram showed a single hydratase activity band on the gel with a molecular weight of about 33.0 kDa, corresponding to the monomeric form of the chimeric EcoCAγ (Figure 5). This was not a surprise since the protonography analysis requires the elimination of SDS at the end of the electrophoretic run. Even if all the γ-CAs are active as trimers, the yellow band appeared in the position of the inactive monomeric form because the SDS purging leads to the rearrangement of the γ-CA monomers in the gel. As a result, EcoCAγ correctly refolded and generated the active trimeric forms of the γ-CA at the position of the monomer. This is described for other eukaryotic and prokaryotic CA classes, too[63]

3.3. Determination of the kinetic parameters using the stopped-flow technique

The CO_2 hydratase activity of the soluble enzyme and its kinetic constants were determined using the stopped-flow technique (Table 1). These results were compared with the kinetic parameters of the two mammalian α-CA isoforms (h CAI and h CAII), as

Table 1. Kinetic parameters for the CO_2 hydration reaction catalysed by the α-, β-, and γ-class CA enzymes: hCA I and II (α-class CAs), and VchCAα at 20 °C and pH 7.5 in 10 mM HEPES buffer; VchCAβ, VchCAγ; CynT2 and EcoCAγ determined at 20 °C, pH 8.3 in 20 mM TRIS buffer and 20 mM NaClO4. Inhibition data with the clinically used sulphonamide AZA (5-acetamido-1,3,4-thiadiazole-2-sulphonamide) are also provided.

Organism	Acronym	Class	k_{cat} (s^{-1})	k_{cat}/K_m (M^{-1} x s^{-1})	K_I (acetazolamide) (nM)
Homo sapiens[a]	hCA I	α	2.0×10^5	5.0×10^7	250
	hCA II	α	1.4×10^6	1.5×10^8	12
Vibrio cholerae[a]	VchCAα	α	8.2×10^5	7.0×10^7	6.8
	VchCAβ	β	3.3×10^5	4.1×10^7	451
	VchCAγ	γ	7.3×10^5	6.4×10^7	473
Escherichia coli	CynT2[b]	β	5.3×10^5	4.1×10^7	227
	EcoCAγ	γ	5.7×10^5	6.9×10^6	248

Mean from 3 different assays by a stopped flow technique (errors were in the range of ±5–10% of the reported values).
[a]From reference (14); [b]From reference (50).

well as with the β-CA from the same microorganism and the α-, β-, and γ- CAs from *Vibrio cholerae* (Table 1).

As shown in Table 1, EcoCAγ is an excellent catalyst for the physiological CO_2 hydratase reaction to bicarbonate and protons, with a k_{cat} of $5.7 \times 10^5 \, s^{-1}$ and catalytic efficiency (k_{cat}/K_M) of $6.9 \times 10^6 \, M^{-1} \, s^{-1}$. EcoCAγ k_{cat} was similar to those obtained for other bacterial CAs belonging to the β-or γ- classes, as well as for the human isoform hCA I. Interestingly, the catalytic efficiency of EcoCAγ resulted to be two orders of magnitude lower with respect to that of hCA II and one order with respect to VchCAγ (same class of EcoCAγ) and the other enzymes reported in Table 1. The investigation of the kinetic properties of the CAs is important because even if these enzymes belong to the same or different CA-classes the steric hindrance of the amino acid residues surrounding the catalytic pocket is responsible for the increase/decrease of the parameters related to the affinity of the enzyme for the substrate (K_M). EcoCAγ was also inhibited by the sulphonamide acetazolamide ($K_I = 248 \, nM$), a well-known pharmacological CA inhibitor (Table 1). The acetazolamide resulted to be a very sensitive inhibitor of the human isoform h CAII ($K_I=12 \, nM$) and the α-CA from *Vibrio cholerae* ($K_I=6.8 \, nM$), wheras for the other CAs reported in Table 1 it was less effective, with K_Is in the range of 227–473 nM. Thus, the K_I variation can be attributed to the interaction and steric hindrance of the amino acid residues of the catalytic pocket interacting with the inhibitor. The structural

differences, which affect the CA-classes or CAs belonging to the same class, highlight the possibility of designing specific and selective inhibitors for this superfamily of enzymes.

3.4. Sulphonamide inhibition profile

Among the CAIs, a library of 42 compounds, **1–24** and **AAZ-EPA,** represent an important group of simple aromatic/heterocyclic sulphonamides (including one sulfamate), which are able to inhibit the CA (Figure 6).

The series **AAZ-EPA** includes licenced drugs used for the following clinical treatments: glaucoma, epilepsy, idiopathic intracranial hypertension, diuretic, duodenal ulcers, migraine, Parkinson's disease, obesity, cancer, osteoarthritis, rheumatoid arthritis, diet, etc.[56–58]. Most of the sulphonamides bind in a tetrahedral geometry to the Zn(II) ion in the deprotonated state, establishing with the amino acid residues of the catalytic site an extended network of hydrogen bonds[18,19,22], as well as the aromatic/heterocyclic part of the inhibitor interacts with the hydrophilic and hydrophobic residues of the catalytic cavity[18,19].

Since CAs are considered a valuable target for impairing the microbe vitality or their virulence, the *in vitro* exploration of the EcoCAγ inhibition profile with such inhibitors is crucial for obtaining potent and selective families of new pharmacological agents. New drugs are needed considering that the emergence arisen
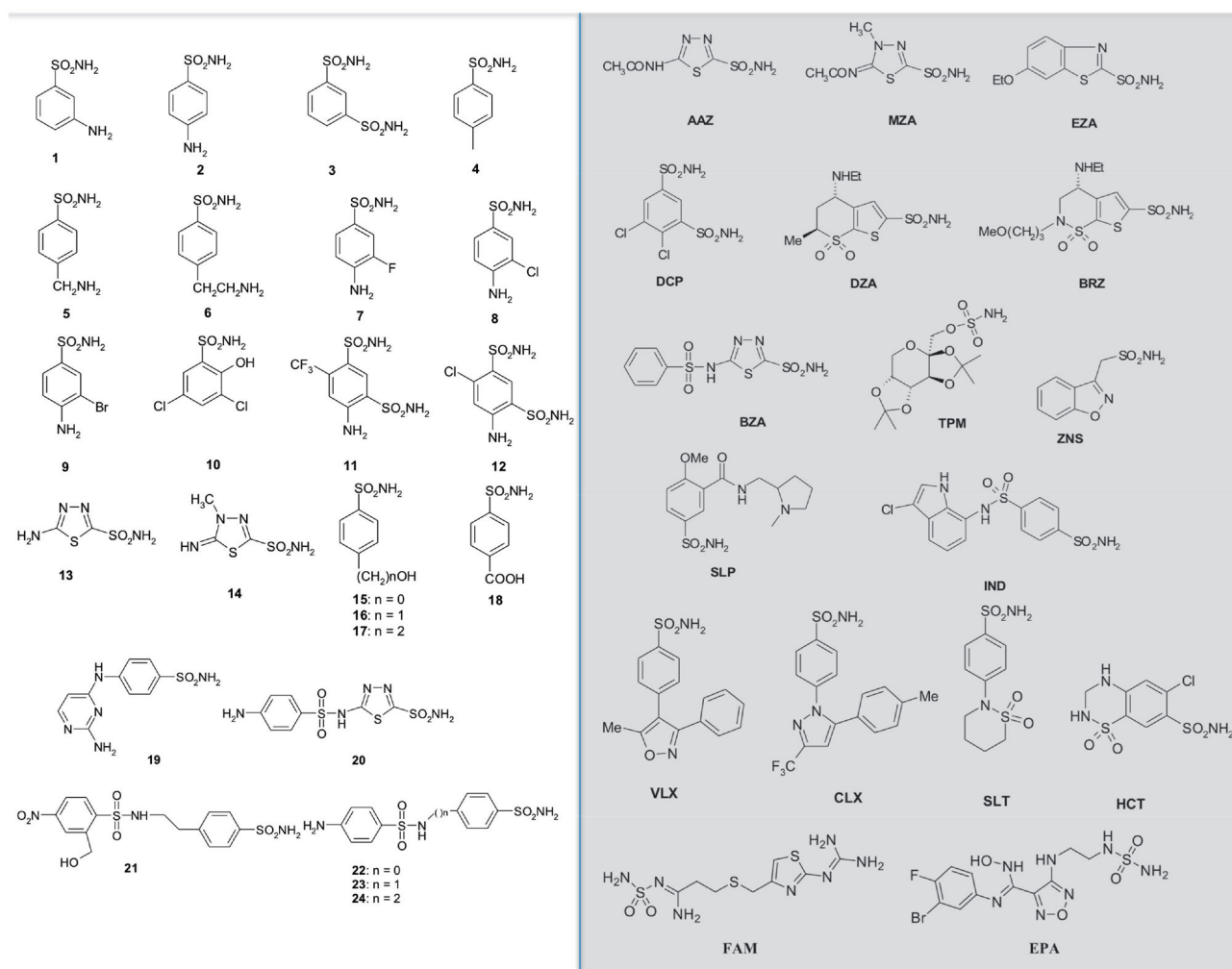

Figure 6. The 42 compounds used to study the EcoCAγ inhibition profile. Forty-one sulphonamides and one sulfamate (TPM) were exploited. On the left, the series 1–24; on the right and grey, the clinically used drugs.

Table 2. Inhibition of hCA I, hCA II, EcoCAγ and VchCAγ with sulphonamides 1–24 and the clinically used drugs **AAZ-EPA**.

Inhibitor	K_I*(nM)			
	hCA I[a]	hCA II[a]	EcoCAγ	VchCAγ [a]
1	28000	300	314	672
2	25000	240	193	95
3	79	8	246	94
4	78500	320	221	76
5	25000	170	160	81
6	21000	160	622	69
7	8300	60	605	74
8	9800	110	671	74
9	6500	40	718	95
10	7300	54	2577	544
11	5800	63	1779	87
12	8400	75	1953	563
13	8600	60	197	66
14	9300	19	712	70
15	5500	80	1013	88
16	9500	94	4238	556
17	21000	125	1975	6223
18	164	46	2064	5100
19	109	33	1894	4153
20	6	2	883	5570
21	69	11	819	764
22	164	46	3501	902
23	109	33	4045	273
24	95	30	4262	73
AAZ	250	12	248	473
MZA	50	14	921	494
EZA	25	8	5538	85
DCP	1200	38	889	1230
DZA	50000	9	2007	87
BRZ	45000	3	4842	93
BZA	15	9	94	78
TPM	250	10	648	69
ZNS	56	35	755	725
SLP	1200	40	914	78
IND	31	15	387	91
VLX	54000	43	891	817
CLX	50000	21	944	834
SLT	374	9	446	464
SAC	18540	5959	4903	550
HCT	328	290	3643	500
FAM	922	58	274	–
EPA	8262	917	744	–

*Errors in the range of 5–10% of the reported data, from 3 different assays (data not shown). [a]Human recombinant isozymes and *Vibro enzyme* stopped flow CO_2 hydrase assay method from ref.[14]; –, not detected.

from the resistance to the existing antimicrobial medicines is one of the most severe problems afflicting the human community. Table 2 reports the inhibition profile of EcoCAγ, which was compared with the inhibitory behaviour of hCA I, hCA II, and VchCAγ reported earlier by our group[17,56,71]. From the data of Table 2, the following can be observed:

1. Among the sulphonamides and sulfamate used to determine the EcoCAγ inhibition profile, only one inhibitor resulted in a K_I lower than 100 nM. This is the case of the benzolamide (**BZA**) whit a $K_I = 94$ nM. Generally, **BZA** is clinically used in the treatment of glaucoma. The two human isoforms, hCA I and hCA II, resulted very sensitive to such inhibitor with a K_I of 15 and 9 nM, respectively. The *Vibrio* enzyme was inhibited with a $K_I = 78$ nM. *V. cholerae* enzyme showed a large number of nanomolar inhibitors with a K_I below 100 nM, such as compounds **2**, **3**, **4**, **5**, **6**, **7**, **8**, **9**, **11**, **13**, **14**, **15**, **24**, **EZA**, **DZA**, **BRZ**, **BZA**, the sulfamate **TPM**, **SLP,** and **IND**. Except for BZA, these inhibitors inhibited EcoCAγ with K_{Is} in the range 193–1013 nM for the series **1–24**, and K_{Is} of 387-5538 nM for

the proposed licenced drugs. The analysis of the three-dimensional structures of EcoCAγ and VchCAγ (not available at this moment) will allow the identification of the structural factors responsible for the K_I variations, and thus the possibility to design efficient and selective inhibitors of the bacterial enzymes.

2. Most of the inhibitors considered in the present study were moderate inhibitors of EcoCAγ with K_{Is} in the range 160–944 nM, such as compounds from **1** to **9**, **13**, **14**, **20**, **21**, **AZA**, **MZA**, **DCP**, **TMP**, **ZNS**, **SLP**, **IND**, **VLX**, **CLX**, **SLT**, **FAM,** and **EPA**. It is important to note that some of these inhibitors were very sensitive versus the human isoform h CAII and harmful inhibitors for the human isoform h CA I (KI = 6.6 – 78.5 μM). The zonisamide (**ZNS**) an aliphatic primary sulphonamide, was also a very weak inhibitor for the bacterial enzymes (K_{Is}= 725 nM) but effective towards the human isoenzymes (K_{Is}= 35–56 nM). The K_I differences reported in the Table 2 evidenced that the inhibition pattern is almost different also between the human isoenzymes corroborating the idea that the comparison of the inhibition profile represents a potent tool for developing new specific inhibitors. For example, it is possible to tune and/or design specific inhibitors for the isoforms based on their structural differences, even if the isoenzymes show a high percentage of amino acid sequence identity.

3. Several substituted benzene-sulphonamides, such as **10**, **11**, **12**, **15**, **16**, **17**, **18**, **19**, **22**, **23**, **24**, **EZA**, **DZA**, and **BRZ**, were ineffective week inhibitors of the EcoCAγ, showing K_{Is} in the range of 1.0–5.5 μM. Moreover, most of these inhibitors, such as the compounds **11**, **24**, **EZA**, **DZA**, and **BRZ**, inhibited the Vibrio enzyme (VchCAγ) with K_{Is} =73–93 nM.

The behaviour of EcoCAγ is somewhat challenging to explain observing the different inhibition profiles and comparing them to the orthologous VchCAγ and the two human isoforms (hCA I and hCA II). EcoCAγ seems less or not inhibited by most of the substituted benzene-sulphonamides and clinically licenced drugs. However, considering that also the two human isoforms showed a sulphonamide inhibition pattern different from each other, as well as from the bacterial enzymes, it is reasonable to support the thesis concerning the synthesis of new drugs capable of interfering selectively with EcoCAγ or VchCAγ activity, avoiding the inhibition of the human CAs (α-class enzymes).

4. Conclusions

Escherichia coli is an opportunistic pathogen typically colonising the lower intestine of warm-blooded organisms[51–54]. In the present manuscript, we focussed our interest on the EcoCAγ (γ-CA) encoded by the *E. coli* genome since bacterial CAs are considered a valuable target for impairing the microbe vitality or the bacterial virulence. EcoCAγ was cloned, expressed, purified, and investigated for its kinetic properties, the last not explored previously even if the three-dimensional structure was solved in 2012 (55). EcoCAγ resulted in an excellent catalyst for the physiological CO_2 hydratase reaction to bicarbonate and protons, with a k_{cat} of $5.7 \times 10^5 \, s^{-1}$ and catalytic efficiency (k_{cat}/K_M) of $6.9 \times 10^6 \, M^{-1} \, s^{-1}$. A broad range of substituted benzene-sulphonamides and clinically licenced drugs were used to determine the inhibition profile of EcoCAγ, the ortholog enzyme VchCAγ, and the possible off-targets hCA I and hCA II. Among the sulphonamides and the one sulfamate used as inhibitors, only one of them resulted in a K_I lower than 100 nM. This is the case of the benzolamide (**BZA**)

whit a $K_I = 94$ nM. Generally, **BZA** is clinically used in the treatment of glaucoma. All the other inhibitors had $K_{Is} > 100$ nM. Surprisingly, for most of the inhibitors used, EcoCAγ showed $0.5 < K_{is} < 0.5\,\mu$M, evidencing that enzyme form *E. coli* was less or not inhibited by most of the substituted benzene-sulphonamides and clinically licenced drugs. As a consequence, the difference in sulphonamide inhibition pattern of the two human isoforms, as well as the two orthologs bacterial enzyme fortifies the thesis that the synthesis of new drugs is capable of interfering selectively with EcoCAγ or VchCAγ activity, avoiding the inhibition of the human CAs (α-class enzymes).

Acknowledgements

Disclosure statement

The authors state no conflict of interests.

ORCID

Sonia Del Prete   http://orcid.org/0000-0001-5291-8823
Claudiu T. Supuran   http://orcid.org/0000-0003-4262-0323
Clemente Capasso   http://orcid.org/0000-0003-3314-2411

References

1. Wang QK. [Responses of forest soil carbon pool and carbon cycle to the changes of carbon input]. Ying Yong Sheng Tai Xue Bao 2011;22:1075–81.
2. Sellers PJ, Schimel DS, Moore B, 3rd, et al. Observing carbon cycle-climate feedbacks from space. Proc Natl Acad Sci USA 2018;115:7860–8.
3. Lettinga G. Digestion and degradation, air for life. Water Sci Technol 2001;44:157–76.
4. Offre P, Spang A, Schleper C. Archaea in biogeochemical cycles. Annu Rev Microbiol 2013;67:437–57.
5. Piao S, Wang X, Wang K, et al. Interannual variation of terrestrial carbon cycle: issues and perspectives. Glob Chang Biol 2020;26:300–18.
6. Atkinson N, Feike D, Mackinder LC, et al. Introducing an algal carbon-concentrating mechanism into higher plants: location and incorporation of key components. Plant Biotechnol J 2016;14:1302–15.
7. Supuran CT, Capasso C. An overview of the bacterial carbonic anhydrases. Metabolites 2017;7:56.
8. Capasso C, Supuran CT. An overview of the alpha-, beta- and gamma-carbonic anhydrases from bacteria: can bacterial carbonic anhydrases shed new light on evolution of bacteria? J Enzyme Inhib Med Chem 2015;30:325–32.
9. Del Prete S, Nocentini A, Supuran CT, Capasso C. Bacterial ι-carbonic anhydrase: a new active class of carbonic anhydrase identified in the genome of the Gram-negative bacterium *Burkholderia territorii*. J Enzyme Inhib Med Chem 2020; 35:1060–8.
10. Del Prete S, De Luca V, De Simone G, et al. Cloning, expression and purification of the complete domain of the η-carbonic anhydrase from *Plasmodium falciparum*. J Enzyme Inhib Med Chem 2016;31:54–9.
11. Del Prete S, Vullo D, De Luca V, et al. Cloning, expression, purification and sulfonamide inhibition profile of the complete domain of the η-carbonic anhydrase from *Plasmodium falciparum*. Bioorg Med Chem Lett 2016;26: 4184–90.
12. Del Prete S, Vullo D, De Luca V, et al. Anion inhibition profiles of the complete domain of the η-carbonic anhydrase from *Plasmodium falciparum*. Bioorg Med Chem 2016;24: 4410–4.
13. Annunziato G, Angeli A, D'Alba F, et al. Discovery of new potential anti-infective compounds based on carbonic anhydrase inhibitors by rational target-focused repurposing approaches. ChemMedChem 2016;11:1904–14.
14. Del Prete S, Vullo D, De Luca V, et al. Anion inhibition profiles of α-, β- and γ-carbonic anhydrases from the pathogenic bacterium *Vibrio cholerae*. Bioorg Med Chem 2016;24: 3413–7.
15. Abdel Gawad NM, Amin NH, Elsaadi MT, et al. Synthesis of 4-(thiazol-2-ylamino)-benzenesulfonamides with carbonic anhydrase I, II and IX inhibitory activity and cytotoxic effects against breast cancer cell lines. Bioorg Med Chem 2016;24: 3043–51.
16. Capasso C, Supuran CT. An overview of the carbonic anhydrases from two pathogens of the oral cavity: *Streptococcus mutans* and *Porphyromonas gingivalis*. Curr Top Med Chem 2016;16:2359–68.
17. Del Prete S, Vullo D, De Luca V, et al. Comparison of the sulfonamide inhibition profiles of the α-, β- and γ-carbonic anhydrases from the pathogenic bacterium *Vibrio cholerae*. Bioorg Med Chem Lett 2016;26:1941–6.
18. Supuran CT. Advances in structure-based drug discovery of carbonic anhydrase inhibitors. Expert Opin Drug Discov 2017;12:61–88.
19. Supuran CT. Structure and function of carbonic anhydrases. Biochem J 2016;473:2023–32.
20. Nishimori I, Onishi S, Takeuchi H, Supuran CT. The alpha and beta classes carbonic anhydrases from *Helicobacter pylori* as novel drug targets. Curr Pharm Des 2008;14:622–30.
21. Morishita S, Nishimori I, Minakuchi T, et al. Cloning, polymorphism, and inhibition of beta-carbonic anhydrase of *Helicobacter pylori*. J Gastroenterol 2008;43:849–57.
22. Supuran CT. How many carbonic anhydrase inhibition mechanisms exist? J Enzyme Inhib Med Chem 2016;31:345–60.
23. De Simone G, Monti SM, Alterio V, et al. Crystal structure of the most catalytically effective carbonic anhydrase enzyme known, SazCA from the thermophilic bacterium *Sulfurihydrogenibium azorense*. Bioorg Med Chem Lett 2015; 25:2002–6.
24. Supuran CT. Carbonic anhydrase inhibition and the management of neuropathic pain. Expert Rev Neurother 2016;16: 961–8.
25. Ozensoy Guler O, Supuran CT, Capasso C. Carbonic anhydrase IX as a novel candidate in liquid biopsy. J Enzyme Inhib Med Chem 2020;35:255–60.
26. Blandina P, Provensi G, Passsani MB, et al. Carbonic anhydrase modulation of emotional memory. Implications for the treatment of cognitive disorders. J Enzyme Inhib Med Chem 2020;35:1206–14.
27. Supuran CT, Capasso C. Biomedical applications of prokaryotic carbonic anhydrases. Expert Opin Ther Pat 2018;28: 745–54.
28. Supuran CT, Capasso C. Carbonic anhydrase from porphyromonas gingivalis as a drug target. Pathogens 2017;6:30.

29. Capasso C, Supuran CT. Bacterial, fungal and protozoan carbonic anhydrases as drug targets. Expert Opin Ther Targets 2015;19:1689–704.

30. Allocati N, Masulli M, Alexeyev MF, Di Ilio C. *Escherichia coli* in Europe: an overview. Int J Environ Res Public Health 2013;10:6235–54.

31. Conway T, Cohen PS. Commensal and pathogenic *Escherichia coli* metabolism in the gut. Microbiol Spectr 2015;3: 23.

32. Robins-Browne RM, Holt KE, Ingle DJ, et al. Are *Escherichia coli* pathotypes still relevant in the era of whole-genome sequencing? Front Cell Infect Microbiol 2016;6:141

33. Guilloton MB, Lamblin AF, Kozliak EI, et al. A physiological role for cyanate-induced carbonic anhydrase in *Escherichia coli*. J Bacteriol 1993;175:1443–51.

34. Kozliak EI, Guilloton MB, Gerami-Nejad M, et al. Expression of proteins encoded by the *Escherichia coli* cyn operon: carbon dioxide-enhanced degradation of carbonic anhydrase. J Bacteriol 1994;176:5711–7.

35. Guilloton MB, Korte JJ, Lamblin AF, et al. Carbonic anhydrase in *Escherichia coli*. A product of the cyn operon. J Biol Chem 1992;267:3731–4.

36. Kusian B, Sultemeyer D, Bowien B. Carbonic anhydrase is essential for growth of *Ralstonia eutropha* at ambient CO(2) concentrations. J Bacteriol 2002;184:5018–26.

37. Cronk JD, Endrizzi JA, Cronk MR, et al. Crystal structure of *E. coli* beta-carbonic anhydrase, an enzyme with an unusual pH-dependent activity. Protein Sci 2001;10:911–22.

38. Merlin C, Masters M, McAteer S, Coulson A. Why is carbonic anhydrase essential to *Escherichia coli*? J Bacteriol 2003;185: 6415–24.

39. Ueda K, Nishida H, Beppu T. Dispensabilities of carbonic anhydrase in proteobacteria. Int J Evol Biol 2012;2012: 324549

40. Modak JK, Tikhomirova A, Gorrell RJ, et al. Anti-*Helicobacter pylori* activity of ethoxzolamide. J Enzyme Inhib Med Chem 2019;34:1660–7.

41. Ronci M, Del Prete S, Puca V, et al. Identification and characterization of the α-CA in the outer membrane vesicles produced by *Helicobacter pylori*. J Enzyme Inhib Med Chem 2019;34:189–95.

42. Buzas GM. [*Helicobacter pylori* – 2010]. Orv Hetil 2010;151: 2003–10.

43. Abuaita BH, Withey JH. Bicarbonate induces *Vibrio cholerae* virulence gene expression by enhancing ToxT activity. Infect Immun 2009;77:4111–20.

44. Kohler S, Ouahrani-Bettache S, Winum JY. *Brucella suis* carbonic anhydrases and their inhibitors: towards alternative antibiotics? J Enzyme Inhib Med Chem 2017;32:683–7.

45. Singh S, Supuran CT. 3D-QSAR CoMFA studies on sulfonamide inhibitors of the Rv3588c β-carbonic anhydrase from Mycobacterium tuberculosis and design of not yet synthesized new molecules. J Enzyme Inhib Med Chem 2014;29: 449–55.

46. Ceruso M, Vullo D, Scozzafava A, Supuran CT. Sulfonamides incorporating fluorine and 1,3,5-triazine moieties are effective inhibitors of three β-class carbonic anhydrases from *Mycobacterium tuberculosis*. J Enzyme Inhib Med Chem 2014; 29:686–9.

47. Carta F, Maresca A, Covarrubias AS, et al. Carbonic anhydrase inhibitors. Characterization and inhibition studies of the most active beta-carbonic anhydrase from

48. Rollenhagen C, Bumann D. *Salmonella enterica* highly expressed genes are disease specific. Infect Immun 2006;74: 1649–60.

49. Lotlikar SR, Kayastha BB, Vullo D, Khanam , et al. Pseudomonas aeruginosa β-carbonic anhydrase, psCA1, is required for calcium deposition and contributes to virulence. Cell Calcium 2019;84:102080.

50. Del Prete S, De Luca V, Nocentini A, et al. Anion inhibition studies of the beta-carbonic anhydrase from *Escherichia coli*. Molecules 2020;25:2564–77.

51. Pitout JD. Extraintestinal pathogenic *Escherichia coli*: a combination of virulence with antibiotic resistance. Front Microbiol 2012;3:9

52. Nataro JP, Kaper JB. Diarrheagenic *Escherichia coli*. Clin Microbiol Rev 1998;11:142–201.

53. Moriel DG, Bertoldi I, Spagnuolo A, et al. Identification of protective and broadly conserved vaccine antigens from the genome of extraintestinal pathogenic *Escherichia coli*. Proc. Natl. Acad. Sci. U.S.A 2010;107:9072–7.

54. Agus A, Massier S, Darfeuille-Michaud A, et al. Understanding host-adherent-invasive *Escherichia coli* interaction in Crohn's disease: opening up new therapeutic strategies. Biomed Res Int 2014;2014:567929.

55. Park HM, Park JH, Choi JW, et al. Structures of the γ-class carbonic anhydrase homologue YrdA suggest a possible allosteric switch. Acta Crystallogr D Biol Crystallogr 2012;68: 920–6.

56. Supuran CT. Carbonic anhydrases: novel therapeutic applications for inhibitors and activators. Nat Rev Drug Discov 2008;7:168–81.

57. Nguyen K, Ahlawat R, Famotidine. Treasure Island (FL): StatPearls; 2020.

58. Komiya T, Huang CH. Updates in the clinical development of epacadostat and other Indoleamine 2,3-Dioxygenase 1 Inhibitors (IDO1) for human cancers. Front Oncol 2018;8:423

59. Del Prete S, Vullo D, Ghobril C, et al. Cloning, purification, and characterization of a beta-carbonic anhydrase from *Malassezia restricta*, an opportunistic pathogen involved in dandruff and seborrheic dermatitis. Int J Mol Sci 2019;20: 2447–58.

60. Bradford MM. A rapid and sensitive method for the quantitation of microgram quantities of protein utilizing the principle of protein-dye binding. Anal Biochem 1976;72:248–54.

61. Capasso C, De Luca V, Carginale V, et al. Biochemical properties of a novel and highly thermostable bacterial α-carbonic anhydrase from *Sulfurihydrogenibium yellowstonense* YO3AOP1. J Enzyme Inhib Med Chem 2012;27:892–7.

62. Laemmli UK. Cleavage of structural proteins during the assembly of the head of bacteriophage T4. Nature 1970;227: 680–5.

63. De Luca V, Del Prete S, Supuran CT, Capasso C. Protonography, a new technique for the analysis of carbonic anhydrase activity. J Enzyme Inhib Med Chem 2015;30: 277–82.

64. Del Prete S, De Luca V, Iandolo E, et al. Protonography, a powerful tool for analyzing the activity and the oligomeric state of the γ-carbonic anhydrase identified in the genome of *Porphyromonas gingivalis*. Bioorg Med Chem 2015;23: 3747–50.

65. Del Prete S, De Luca V, Supuran CT, Capasso C. Protonography, a technique applicable for the analysis of

Mycobacterium tuberculosis, Rv3588c. Bioorg Med Chem Lett 2009;19:6649–54.

η-carbonic anhydrase activity. J Enzyme Inhib Med Chem 2015;30:920–4.

66. Del Prete S, Vullo D, Caminiti-Segonds N, et al. Protonography and anion inhibition profile of the α-carbonic anhydrase (CruCA4) identified in the Mediterranean red coral *Corallium rubrum*. Bioorg Chem 2018;76:281–7.

67. Khalifah RG. The carbon dioxide hydration activity of carbonic anhydrase. I. Stop-flow kinetic studies on the native human isoenzymes B and C. J Biol Chem 1971;246:2561–73.

68. De Luca V, Vullo D, Del Prete S, et al. Cloning, characterization and anion inhibition studies of a γ-carbonic anhydrase from the *Antarctic bacterium Colwellia psychrerythraea*. Bioorg Med Chem 2016;24:835–40.

69. Bossy R, Golik W, Ratkovic Z, et al. Overview of the gene regulation network and the bacteria biotope tasks in BioNLP'13 shared task. BMC Bioinformatics 2015;16:S1.

70. Fu X, Yu LJ, Mao-Teng L, et al. Evolution of structure in gamma-class carbonic anhydrase and structurally related proteins. Mol Phylogenet Evol 2008;47:211–20.

71. Angeli A, Ferraroni M, Supuran CT. Famotidine, an antiulcer agent, strongly inhibits *Helicobacter pylori* and human carbonic anhydrases. ACS Med Chem Lett 2018;9:1035–8.